THE ROTATION VELOCITY - DENSITY RELATION

Lorraine A. Allen and Margaret J. Geller
Harvard-Smithsonian Center for Astrophysics

ABSTRACT

We have assembled 21-cm linewidths for 376 of the 732 galaxies in a magnitude-limited redshift survey of the Perseus-Pisces region.

We analyze a distance limited subset of 271 galaxies (131 widths) to examine the relationship between linewidth and local density. The sample indicates that galaxies with linewidths $\gtrsim 480$ km/s are absent from regions where the galaxy density is $\lesssim 0.03$ galaxies Mpc^{-3} ($M_{B(0)} < -18.3$). This effect is in the direction predicted by standard CDM models. Galaxies with linewidths $\lesssim 480$ km/s appear throughout the sample.

The observational constraints could be susbtantially improved with a larger sample, IR photometry, and more uniform 21-cm data.

1. Introduction

Cold Dark Matter (CDM) models are the most successful in accounting for the observed properties of large scale structure in the universe (see Ostriker 1993 for a review; Zurek *et al.* 1994, Ueda *et al.* 1994). Biased CDM models, in which galaxies are more clustered than the overall mass distribution, can account for the observed galaxy clustering on scales $\lesssim 10h^{-1}$ Mpc, rms peculiar velocities of galaxies, and the qualitative appearance of large scale features - voids, filaments, and walls (White *et al.* 1987b, Park 1990, Cen and Ostriker 1992). In addition, these models descibe many of the properties of individual galaxies, including dark haloes around spirals with flat rotation curves; they also provide an explanation for the formation of the different morphological types and for the observed morphology-density relation (Cen and Ostriker 1993, Frenk *et al.* 1985).

CDM models with $\Omega h = 1/2$ fail to account for the observed galaxy distribution on large scales $\gtrsim 30h^{-1}$ Mpc (Park *et al.* 1994, Ueda *et al.* 1993, Gelb and Bertschinger 1994). The models also fail to account for observed large scale flows (White *et al.* 1987b, Strauss *et al.* 1995). Minimally biased low-density CDM models with $\Omega h \simeq 0.2 - 0.3$ (with and without a non-zero cosmological constant) are consistent with the large-scale galaxy distribution and with the amplitude of mass fluctuations at the current epoch implied by COBE (Kofman *et al.* 1993, Ueda *et al.* 1993, Park *et al.* 1994, Cen and Ostriker 1994).

Galaxy formation in biased CDM models occurs preferentially in regions where the density exceeds a threshold. In all CDM models, the most massive galaxies tend to form in the densest regions; here the matter collapses and accretes more rapidly than at lower density. Furthermore,

high density regions cluster (thus galaxies are more clustered than the overall mass distribution) and thus the most massive galaxies tend to be more clustered. Simulations of CDM models demonstrate these effects (White *et al.* 1987a, Cen and Ostriker 1993, Evrard *et al.* 1994).

Because mass and luminosity are correlated, the models predict luminosity segregation. In other words, the brightest galaxies should be preferentially in the densest regions. Park *et al.* (1994) observed this effect in the CfA survey at about the 2σ level. Davis *et al.* (1988) found, based on correlation functions for the CfA1 and Southern Sky surveys, that brighter galaxies cluster more than fainter ones. Similarly, Gramann and Einasto (1992) claim that bright galaxies preferentially populate high-density regions in the Virgo, Coma, and Perseus superclusters on scales $3 - 20\ h^{-1}$ Mpc.

Rotation velocity is a more direct and cleaner indicator of mass than is the luminosity; thus, it should also be a function of local galaxy density. The rotation velocity ΔV and the luminosity, L, obey the Tully-Fisher relation, $L \propto \Delta V^{\beta}$ where $\beta = 2 - 4$ depending on color; $\beta \simeq 2$ at B with large scatter. The scatter at B results largely from internal extinction in the galaxies (Aaronson *et al.* 1979). Examining the correlation between rotation velocity and local galaxy density is a more direct constraint on CDM models than a relationship between luminosity and local density.

So far, White *et al.* (1988) have made the only attempt to assess the rotation velocity-local density relation. They analyzed a sample of 1387 galaxies from the NGC and found a correlation between rotation velocity and density consistent with CDM. However, only about one third of the galaxies have measured linewidths; most of the widths are actually derived from Tully-Fisher relations based on B magnitudes from the NGC. The large scatter in the Tully-Fisher relation at B diminishes the impact of using the rotation velocities. Their sample is also affected by incompleteness and by the relatively large peculiar motions within the Local Supercluster.

Here we examine the relationship between rotation velocity and local galaxy density for a complete sample of 376 galaxies with measured HI linewidths; the sample is in the Perseus-Pisces supercluster region and is deep enough that Virgo infall is not an issue.

Section 2 describes the dataset and tests for systematic bias and incompleteness. In Section 3 we use a nearest neighbor statistic to evaluate the relationship between linewidth and local galaxy density. We conclude in Section 4 and discuss the prospects for improved constraints.

2. The Data

We have assembled 21-cm linewidth measurements (Giovanelli and Haynes 1985 (PP1), Giovanelli *et al.* 1986 (PP2), Giovanelli and Haynes 1989 (PP4), Giovanelli and Haynes 1993 (PP6), Wegner *et al.* 1993 (PP5), Haynes and Giovanelli 1984 (IG4), Huchtmeier and Richter 1989, Eder *et al.* 1991 (EGH), Scodeggio and Gavazzi 1993 (SG), Lu *et al.* 1988 (LHGRL)) for 376 of the 732 galaxies in a magnitude-limited redshift survey of the Perseus-Pisces region. Here

we describe the dataset and examine it for systematic biases.

2.1. Linewidths for a Redshift Survey

The Center for Astrophysics redshift survey (Geller and Huchra 1989, Huchra *et al.* 1990, Huchra *et al.* 1983, Vogeley 1993) covers large regions of the northern and southern galactic hemispheres to a limiting magnitude $m_{Zw} = 15.5$ in the Zwicky (1961-1968) catalog. Here we consider the subsample of 732 galaxies in the southern galactic hemisphere with $cz \leq 8500$ km s^{-1} and with right ascension $22^h < \alpha < 3^h$ and declination $15° \leq \delta < 33°$ (the MLS hereafter). This region minimizes the effect of Galactic obscuration and maximizes the completeness of the sample of galaxies with known linewidth.

We assembled 21-cm linewidths for 376 of the galaxies in the redshift survey (the MLWS hereafter). Giovanelli and Haynes (PP1, PP2, PP4, PP5, PP6, IG4) measured 370 of these linewidths at Arecibo. The other 6 linewidths are from the literature (EGH, SG) or from the Huchtmeier-Richter Catalog (1989). 372 of the measurements are 50% linewidths, 2 are 20% measurements, and 2 measurements are averages of the 50% and 20% widths. All linewidths are corrected for inclination and for redshift broadening. We include only galaxies with inclination $i \geq 40°$. Among the galaxies with measured linewidths, 288 are spirals, 39 are S0 or S0/a, and 49 are irregular, peculiar, or unclassifiable.

HI profiles for 142 of the 376 galaxies are published (PP1, PP2, IG4, EGH, LHGRL, SG, Haynes 1981, Hewitt *et al.* 1983). Of these, 105 profiles are clean, steep-sided profiles with flat baselines. The remaining profiles, because of shallowness or curved baselines, may yield linewidths with larger errors. However, because we do not have a complete set of profiles, we use all of the data.

2.2. Tests for Incompleteness and Systematic Bias

The MLS is a complete magnitude limited survey. Here we examine the completeness of the MLWS and we test for biases in the magnitude and redshift distributions relative to those for the MLS.

For the MLS sample as a whole, we do not have morphological types. However, all 211 MLS galaxies with $m_{Zw} \leq 14.5$ have types (Huchra *et al.* 1983). Of these, 113 galaxies are spirals; 76 of these spirals, 36% of the entire 211 galaxy sample, have $i \geq 40°$ and are contained within the MLWS. Assuming that the morphological composition and orientation of galaxies of the samples are independent of the magnitude limit, the MLS should likewise contain $\sim 36\%$, or 264, spirals with $i \geq 40°$; the MLWS contains 288 spirals, 39% of the MLS sample, in reasonable agreement with expectation.

If galaxies were randomly oriented we would expect to find 42% of spirals with $i \geq 40°$. Because galaxies are apparently fainter when they are more edge-on, the fraction of edge-on galaxies in a magnitude limited sample should be systematically low. The fractions of edge-on spirals are systematically low in both the MLS and the MLWS, but the bias is $\lesssim 2\sigma$ where σ is the $\sqrt{N}$ error in the count. We do not model this bias because the error in the model is likely to exceed the amplitude of the bias.

Figure 1 shows the distribution of MLWS galaxies within the MLS survey in two 9° declination slices. Because of the well-known morphology-density relation, (Dressler 1980, Postman and Geller 1984), the MLWS galaxies are less common in the cores of clusters than in lower density regions. Figures 2a and 2b show the ratio of MLWS to MLS galaxies as a function of apparent magnitude and redshift, respectively. There is no apparent bias as a function of apparent magnitude; in figure 2a all galaxies with $m_{Zw} \leq 13.0$ are in the first bin. The distribution as a function of redshift again reflects the morphology-density relation. In the low density void at $cz \lesssim 4000$ km s^{-1}, the MLWS fraction is somewhat larger than in the Perseus Pisces supercluster at $cz \simeq 5000$ km s^{-1}.

From this set of comparisons we conclude that the MLWS is remarkably free of systematic biases relative to the MLS. The MLS itself may contain biases, but unless these biases are correlated in some way with linewidth, they should not affect the analyses here.

Figure 3 shows the Tully-Fisher (TF) relation for the sample. The squares are the quartile of MLWS galaxies with the largest widths; the triangles are the lowest quartile. The lowest linewidth galaxies are especially faint; for these objects the Tully-Fisher relation is not linear (see Mould *et al.* 1989 and references therein). Aaronson *et al.* (1986) found that a quadratic form of the relation (in the IR) fit their data well. This non-linearity of the TF relation, along with increased scatter in the blue band TF relation, may account for the data in figure 3.

Because the smallest linewidth galaxies are so faint, they are naturally missing from the MLWS at larger redshifts. The brightest galaxies with the largest linewidths are visible throughout the sample region.

3. The Correlation of Linewidth with Local Density

Here we examine the correlation of linewidth with local galaxy density. To avoid binning and thus make use of each linewidth measurement as an independent estimator of the linewidth-density relation, we compute the local density by identifying the N nearest neighbors of each MLWS galaxy. Dressler (1980) and Dressler and Shectman (1988) used this method to examine the morphology-density relation and to investigate velocity substructure within clusters of galaxies.

3.1. The Nearest Neighbor Density Estimator

The density in the neighborhood of the MLWS galaxy is

$$\rho/\rho_{avg} = \frac{N}{\frac{8}{3}\pi D^3 \int_{-\infty}^{M_g} \Phi(M) dM} \tag{1}$$

where D is the median projected distance to the N (=10) nearest neighbors; N=10 provides a stable estimate of the density for the MLWS galaxies. $\Phi(M)$ is the luminosity function for the sample and M_g is

$$M_g = m_{lim} - 25 - 5\log(V_g/H_\circ) \tag{2}$$

where m_{lim} is the magnitude limit and V_g is the MLWS galaxy velocity. The integral in the denominator corrects the galaxy density for the unseen portion of the luminosity function in a magnitude limited sample.

We compute the projected separation between galaxies:

$$D = \sin(\theta/2)(V_g + V_i)/H_\circ, \tag{3}$$

where V_g and V_i are the velocities of the two galaxies in the pair (the subscript g refers to the central MLWS galaxy), θ is their angular separation, and $H_\circ$ is the Hubble constant. We take $H_\circ = 100$ km/s/Mpc throughout. We also require that the velocity difference between the MLWS galaxy and each of its nearest neighbors is less than a cutoff value, V_L. To account for the magnitude limiting, we scale V_L as

$$V_L = V_\circ \left[\int_{-\infty}^{M_{lim}} \Phi(M) dM / \int_{-\infty}^{M_g} \Phi(M) dM \right]^{1/3}, \tag{4}$$

(Huchra & Geller 1982) where M_{lim} is the faintest absolute magnitude at which galaxies in a sample with magnitude limit m_{lim} are visible at fiducial velocity V_F. M_{lim} is then

$$M_{lim} = m_{lim} - 25 - 5\log(V_F/H_\circ) \tag{5}$$

and M_g is given by Eq.(2). $V_\circ$ in Eq.(4) is 1000 km/s with $V_F = 8000$ km/s (Eq. (5)). The resulting values of V_L prevent clipping of the velocity dispersion of rich clusters but they are not so large that we cross the $\sim$ 5000 km/s voids in the survey. Varying $V_\circ$ by $\sim$30% produces a negligible effect on the local densities.

For a distance-limited sample, we compute the local density

$$\rho/\rho_{avg} = \frac{N}{\frac{8}{3}\pi D^3 \int_{-\infty}^{M_{lim}} \phi(M) dM} \tag{6}$$

where M_{lim} is given by Eq.(5) with $V_F = 1000$ km/s. The corresponding V_L is constant at 800 km/s, comparable with the typical velocity dispersion of a cluster. Again the density estimates

are insensitive to changes in V_L. In contrast with Eq.(1) for the magnitude limited sample, the integral in the denominator is constant here.

Figure 4a shows the correlation between linewidth and density for the nearest neighbor estimator applied to the magnitude limited MLWS. Squares are the highest density quartile; triangles are the lowest. Spearman's rank correlation coefficient is 0.210, a 3.9×10^{-3}% probability of no correlation. Galaxies with linewidths $\gtrsim 480$ km/s preferentially occupy denser regions: there is an absence of these galaxies in the least dense regions in figure 4a.

At the largest densities, the most massive galaxies are early type. The absence of these galaxies from the sample with measured linewidths actually surpresses the correlation. This effect is most evident for $\rho/\rho_{avg} > 2$ and $\Delta V > 620$ km s^{-1}.

Figure 5a shows the distribution of linewidths for the MLWS galaxies with surrounding density in the lowest and highest quartiles. There is a clear shift of the linewidth distribution toward larger linewidth at larger density. The median linewidth is 316^{+92}_{-77} km/s for the lower quartile and 400^{+72}_{-89} km/s for the upper quartile. The errors are the interquartile range for each distribution. A K-S test on the unbinned data for figure 5a shows that there is < 0.04% chance that they are drawn from the same distribution.

The behavior of the galaxies with the smallest linewidths is hard to assess from this sample. The void region at $cz \lesssim 4000$ km/s and the Perseus Pisces supercluster at $cz \simeq 5000$ km/s introduce an artificial correlation between redshift and density. (The Spearman rank coefficient is 0.248). The Tully-Fisher relation (figure 3) implies that galaxies with small linewidths tend to be faint. They are therefore not visible in our magnitude-limited sample at the higher redshifts where the sample is denser.

To remove the artificial correlation between redshift and density and thus to investigate the distribution of small linewidth galaxies with local density, we construct a distance-limited sample, ABS1, with velocity $cz \leq 5700$ km/s and $M_{B(0)} \leq -18.3$. We make this choice to maximize the number of galaxies with known widths: we have 271 galaxies; 131 have measured widths. Because this sample is more sparse than the magnitude-limited MLWS, we choose the number of nearest neighbors for the ABS1 sample which best approximates the density estimates for the entire MLWS sample. The choice N=8 satisfies this criterion.

Figure 4b shows the results for ABS1. The squares are the highest density quartile; the triangles are the lowest quartile. The r_s value is 0.117, an 18.4% probability of no correlation. The galaxies with large linewidths ($\gtrsim 480$ km/s) are absent from regions with log $(\rho/\rho_{avg}) \lesssim -0.4$. There is no such effect for galaxies with small linewidths ($\lesssim 350$ km/s).

Figure 5b shows the distribution of linewidths for galaxies in ABS1 with surrounding densities in the lowest and highest quartiles. The linewidth distribution again shifts toward larger linewidth for galaxies in regions of larger local density. The median linewidth for galaxies in regions of smallest and largest densities are, respectively, 340^{+99}_{-60} and 411^{+72}_{-79} km/s, where the quoted error

is the interquartile range. The difference between the two linewidth distributions for the highest and lowest density regions is significant at roughly the 1.2σ level; a K-S test on the unbinned data for figure 5b shows that there is 14.3% probability that they are drawn from the same distribution. This estimate of significance is probably conservative; figure 4b shows that the first quartile contains some galaxies with large linewidth. The small sample size and the dangers of *a posteriori* statistics prevent us from further dividing the sample, which would probably increase the significance.

Figures 6a and 6b provide strong qualitative support for the absence of galaxies with large linewidth from low density regions: the figures show the distribution in redshift space of the quartile of ABS1 galaxies with the largest and smallest widths, respectively. The squares and triangles are the largest and smallest ABS1 quartile galaxies, respectively, and the crosses are the remaining galaxies in the sample (with and without widths). Figure 6a shows that the galaxies with the largest linewidths occupy the densest regions and are absent from the voids. However (Figure 6b), the smallest linewidth galaxies appear in the voids as well as in higher density regions.

In summary, galaxies in the MLWS of all linewidths populate regions with $\log \rho/\rho_{avg} \gtrsim 0.5$ ($\rho \gtrsim 0.18\ Mpc^{-3}$). However, underdense regions, with $\log \rho/\rho_{avg} \lesssim 0.1$ ($\rho \lesssim 0.07\ Mpc^{-3}$), are deficient in galaxies with linewidths $\gtrsim 480$ km/s.

The effect we find is analogous to the luminosity segregation observed by Park *et al.* (1994) in which galaxies of all luminosities occupy moderate and high density regions; the brightest galaxies are absent from the lowest density regions. For local densities $\rho < 0.015h^3 Mpc^{-3}$ the fraction of bright galaxies is $\simeq 2\sigma$ smaller than expected for a random sample; the bright galaxy fraction is consistent with random for densities $\rho > 0.03h^3 Mpc^{-3}$ ($M_{B(0)} < -19.1$).

As a consistency check for our ABS1 sample, we plot M_{abs} as a function of density, ρ, in figure 7 (compare figure 12 in Park *et al.* (1994)). Open squares represent the quartile with the largest widths; solid triangles are the lowest quartile. At the largest densities, the brightest galaxies are generally absent because early type galaxies are not included in the sample of galaxies with measured linewidths. A subtle luminosity segregation appears in our sample at densities $\lesssim 0.03h^3 Mpc^{-3}$; the effect is less pronounced than in Park *et al.* (1994) because of our smaller sample size. This luminosity segregation is a natural consequence of the dependence of the Tully-Fisher relation (figure 3). However, because of the large scatter in the TF relation (especially at small linewidth), the direct rotation velocity - density relation is the physical relation we seek.

4. Discussion

Our analysis of a distance limited sample of 271 galaxies (131 have measured linewidths) provides evidence for a dependence of linewidth on local galaxy density. The sample indicates that galaxies with linewidths $\gtrsim 480$ km/s are absent from regions where the galaxy density is $\lesssim 0.03$ galaxies Mpc^{-3} ($M_{B(0)} < -18.3$). This effect is in the direction predicted by CDM models.

The analysis of this small sample suggests that the linewidth-local density relation could provide interesting constraints on models for galaxy formation and large-scale structure. The observational constraints could easily be improved by increasing the sample size. Figures 4 and 5 show that even doubling the sample size would provide far more convincing evidence of the absence of galaxies with large linewidth in the lowest density regions.

An important limitation of our analysis is the use of B magnitudes from Zwicky (1961-1968). These data are not of uniform quality and the Tully-Fisher relation at B is broad. A much more powerful test of the linewidth-local density relation could be made with uniform IR photometry. An unbiased set of steep-sided 21cm profiles at high signal-to-noise would also contribute to tighter constraints. On the theoretical side, it would be useful to compute the behavior of the rotation velocity-density relation in terms of the observable parameters.

We thank Riccardo Giovanelli for providing data in a computer readable form. We also thank Antonaldo Diaferio, Emilio Falco, and Michael Kurtz for detailed comments on the manuscript. Lorraine Allen was partially supported by a NASA Graduate Fellowship. This research was supported in part by NASA Grant NAGW-201 and by the Smithsonian Institution.

REFERENCES

Aaronson, M., Mould, M., and Huchra, J. (1979). *Astrophys. J.* **229**, 1.

Aaronson, M., Bothun, G., Mould, J., Huchra, J., Schommer, R., and Cornell, M. (1986). *Astrophys. J.* **302**, 536.

Cen, R. and Ostriker, J. (1992) *Astrophys. J.* **393**, 22.

Cen, R. and Ostriker, J. P. (1993) *Astrophys. J.* **417**, 415.

Cen, R. and Ostriker, J. P. (1994) *Astrophys. J.* **429**, 4.

Davis, M., Meiksin, A., and Strauss, M. A. (1988). *Astrophys. J. Lett.* **333**, L9.

Dressler, A. (1980). *Astrophys. J.* **236**, 351.

Dressler, A., and Schectman, S. A. (1988). *Astron. J.* **95**, 985.

Eder, J., Giovanelli, R., and Haynes, M. P. (1991). *Astron. J.* **102**, 572 (EGH).

Evrard, A. E., Summers, F. J., and Davis, M. (1994). *Astrophys. J.* **422**, 11.

Frenk, C. S., White, S. D. M., Efstathiou, G., and Davis, M. (1985). *Nature* **317**, 595.

Gelb, J. M. and Bertschinger, E. (1994) *Astrophys. J.* **436**, 491.

Geller, M. J., and Huchra, J. P. (1989). *Science* **246**, 897.

Giovanelli, R., and Haynes, M. P. (1993). *Astron. J.* **105**, 1271 (PP6).

Giovanelli, R., and Haynes, M. P. (1989). *Astron. J.* **97**, 633 (PP4)

Giovanelli, R., and Haynes, M. P. (1985). *Astron. J.* **90**, 2445 (PPI).

Giovanelli, R., Haynes, M. P., Myers, S. T., and Roth, J. (1986). *Astron. J.* **92**, 250 (PP2).

Gramann, M. and Einasto, J. (1992). *Mon. Not. R. Astron. Soc.* **254**, 453.

Haynes, M. P. (1981). *Astron. J.* **86**, 1126.

Haynes, M. P., and Giovanelli, R. (1984). *Astron. J.* **89**, 758 (IG4).

Hewitt, J. N., Haynes, M. P., and Giovanelli, R. (1983). *Astron. J.* **88**, 272.

Huchra, J. P., Davis, M., Latham, D., and Tonry, J. (1983). *Astrophys. J. Suppl.* **52**, 89.

Huchra, J. P., and Geller, M. J. (1982). *Astrophys. J.* **257**, 423.

Huchra, J. P., Geller, M. J., deLapparent, V., and Corwin, H. G. (1990). *Astrophys. J. Suppl.* **72**, 433.

Huchtmeier, W. K., and Richter, O.-G. (1989). *A General catalogue of HI Observations of Galaxies* (Springer, New York).

Kofman, L. A., Gnedin, N. Y., and Bahcall, N. A. (1993). *Astrophys. J.* **413**, 1.

Lu, N. Y., Hoffman, G. L., Groff, T., Roos, T., and Lamphier, C. (1993). *Astrophys. J. Suppl.* **88**, 383 (LHGRL).

Marzke, R. O., Geller, M. J., and Huchra, J. P., Corwin, H. G. (1994). *Astron. J.* **108**, 437.

Mould, J., Han, M., and Bothun, G. (1989). *Astrophys. J.* **347**, 112.

Ostriker, J. P. (1993). *Mon. Not. R. Astron. Soc.* **31**, 689.

Park, C. (1990). *Mon. Not. R. Astron. Soc.* **242**, 59P.

Park, C., Vogeley, M. S., Geller, M. J., and Huchra, J. P. (1994). *Astrophys. J.* **431**, 569.

Postman, M. and Geller, M. J. (1984). *Astrophys. J.* **281**, 95.

Scodeggio, M. and Gavazzi, G. (1993). *Astrophys. J.* **409**, 110 (SG).

Strauss, M. A., Cen, R., Ostriker, J. P., Lauer, T. R., and Postman, M. (1995). *Astrophys. J.* **444**, 507.

Ueda, H., Shimasaku, K., Suginohara, T., and Suto, Y. (1994). *Publ. Astron. Soc. Japan* **46**, 319.

Ueda, H., Itoh, M., and Suto, Y. (1993). *Astrophys. J.* **408**, 3.

Vogeley, M. S. (1993). Ph.D. thesis, Harvard University.

Wegner, G., Haynes, M. P., and Giovanelli, R. (1993). *Astron. J.* **105**, 1251 (PP5).

White, S. D. M., Davis, M., Efstathiou, G., and Frenk, C. S. (1987a). *Nature* **330**, 451.

White, S. D. M., Frenk, C. S., Davis, M., and Efstathiou, G. (1987b). *Astrophys. J.* **313**, 505.

White, S. D. M., Tully, R. B., and Davis, M. (1988). *Astrophys. J. Lett.* **333**, L45.

Zurek, W. H., Quinn, P. J., Salmon, J. K., and Warren, M. S. (1994). *Astrophys. J.* **431**, 559.

Zwicky, F., Herzog, E., Karpowicz, M., Kowal, C. T., and Wild, P. (1961-1968). *Catalogues of Galaxies and Clusters of Galaxies* (California Institute of Technology, Pasadena).

Figure Captions

FIG. 1. The distribution of MLWS galaxies (squares) among the MLS galaxies (crosses) in two 9° declination slices.

FIG. 2. a) The ratio of MLWS to MLS galaxies as a function of apparent magnitude. All galaxies with $m_{Zw} \leq 13.0$ are in the first bin. **b)** The ratio of MLWS to MLS galaxies as a function of redshift. The parentheses contain the number of MLWS/MLS galaxies.

FIG. 3. The Tully-Fisher relation for the MLWS. Squares are the quartile of the MLWS with the largest widths; triangles are the lowest quartile.

FIG. 4. a) Linewidth as a function of density (ρ/ρ_{avg}), computed using the Nearest Neighbor Density estimator (N=10), for the MLWS. Squares are the quartile of the MLWS with the largest widths; triangles are the lowest quartile. **b)** Linewidth as a function of density for the ABS1 galaxies. N=8 for the density estimator. Squares and triangles are the quartiles of ABS1 galaxies with the largest and smallest widths, respectively.

FIG. 5. a) The distribution of linewidths for galaxies in the MLWS with densities in the lowest and highest quartiles of the density distribution. The median linewidth for the lower and upper linewidth distributions are, respectively, 316^{+92}_{-77} and 400^{+72}_{-89}, where the quoted error is the interquartile range. **b)** The distribution of linewidths for ABS1 galaxies with densities in the lowest and highest quartiles of the density distribution. The median linewidth for the lower and upper distributions are, respectively, 340^{+99}_{-60} and 411^{+72}_{-79}.

FIG. 6a. The distribution in redshift space of the quartile of ABS1 galaxies with the largest linewidths (squares) among the remaining galaxies (with and without widths) (crosses).

FIG. 6b. The distribution in redshift space of the quartile of ABS1 galaxies with the smallest linewidths (triangles) among the remaining galaxies (with and without widths) (crosses).

FIG. 7. Absolute (blue) magnitude as a function of density, ρ, for the ABS1 sample. Open squares are the quartile of galaxies with the largest linewidths; solid triangles are the lowest quartile.

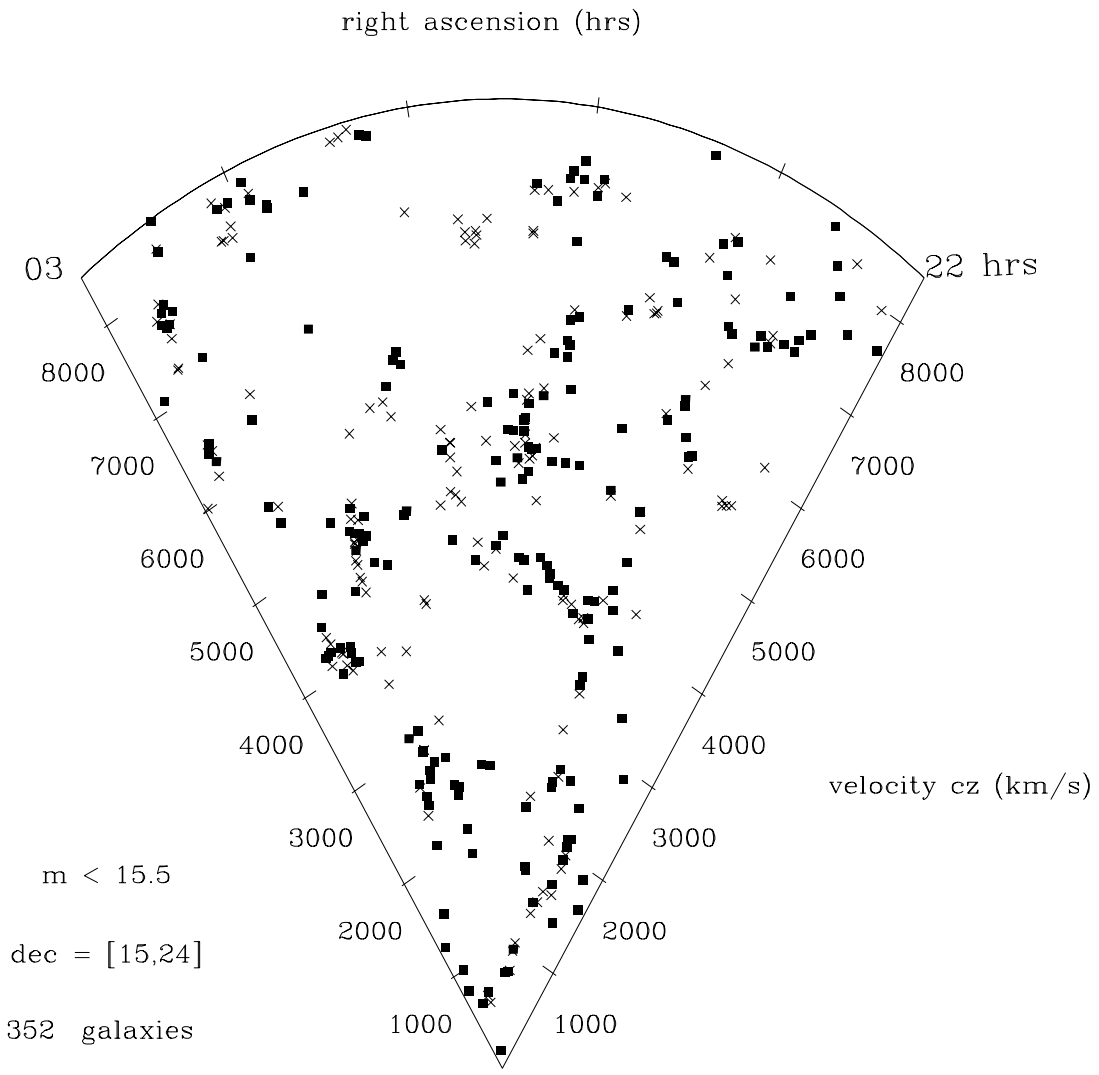
right ascension (hrs)
03
22 hrs
8000
7000
6000
5000
4000
3000
2000
1000
velocity cz (km/s)
m < 15.5
dec = [15,24]
352 galaxies

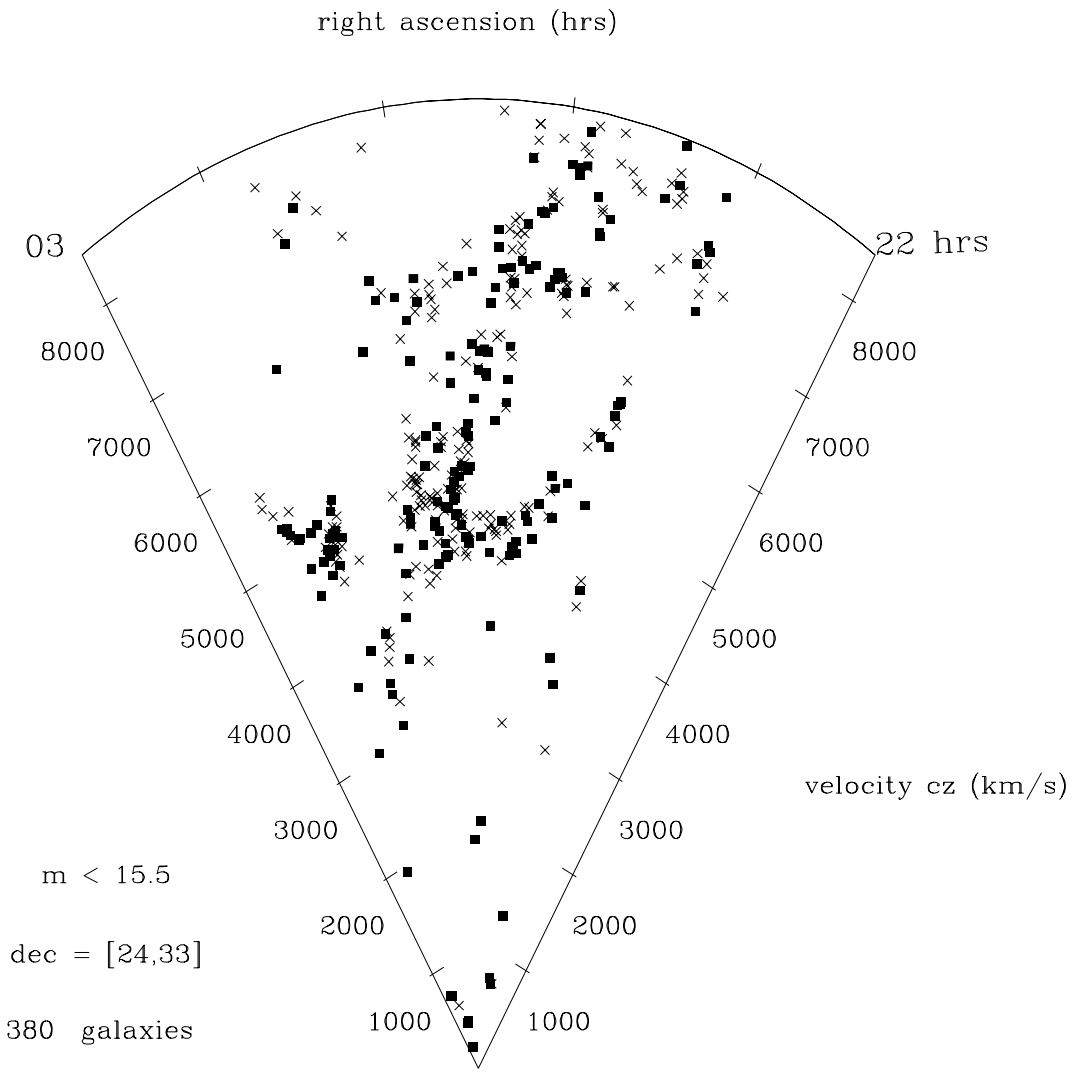
right ascension (hrs)
03
22 hrs
8000
7000
6000
5000
4000
3000
2000
1000
velocity cz (km/s)
m < 15.5
dec = [24,33]
380 galaxies

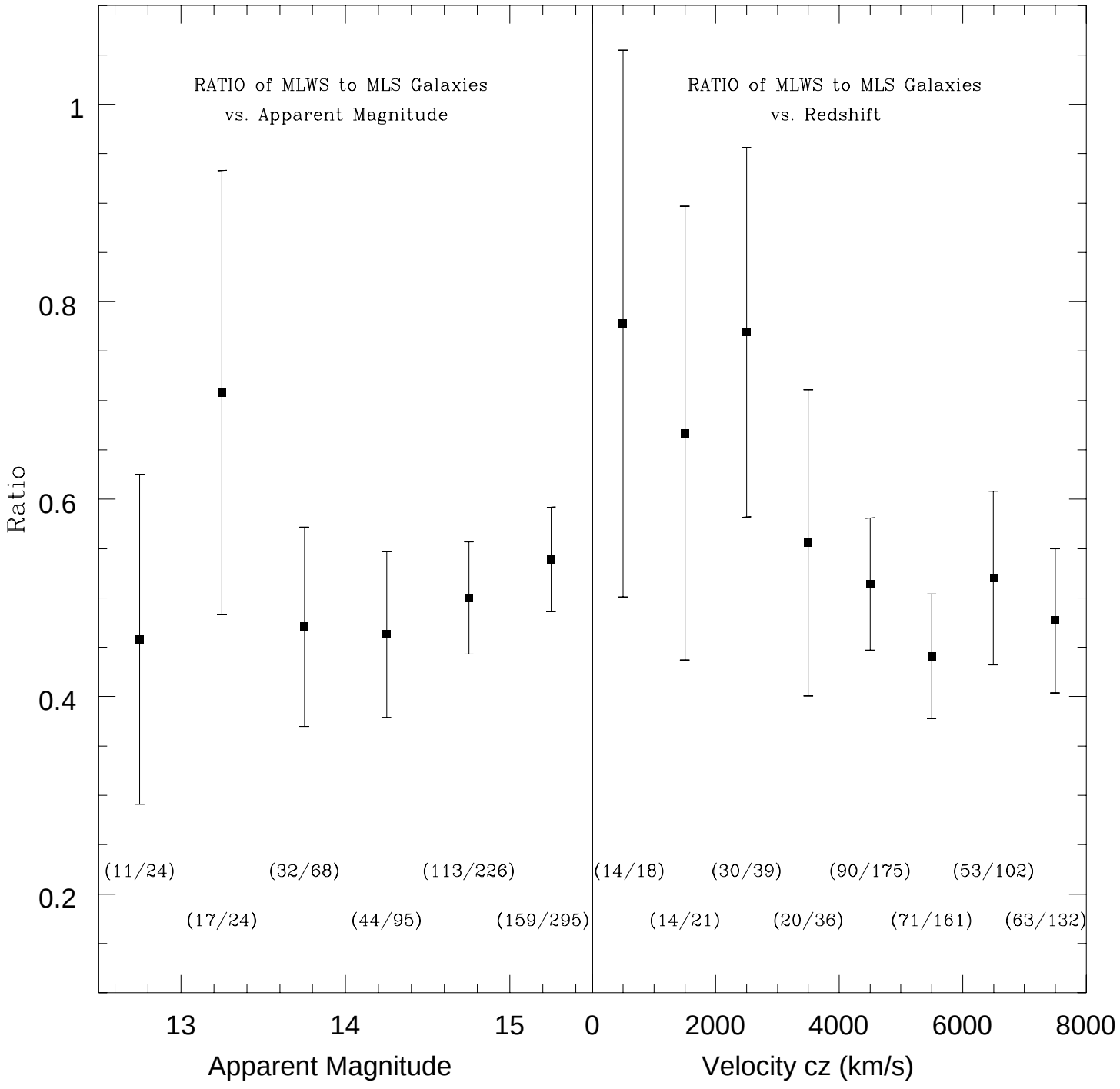
RATIO of MLWS to MLS Galaxies
vs. Apparent Magnitude
RATIO of MLWS to MLS Galaxies
vs. Redshift
Ratio
1
0.8
0.6
0.4
0.2
(11/24)
(17/24)
(32/68)
(44/95)
(113/226)
(159/295)
(14/18)
(14/21)
(30/39)
(20/36)
(90/175)
(71/161)
(53/102)
(63/132)
13
14
15
0
2000
4000
6000
8000
Apparent Magnitude
Velocity cz (km/s)

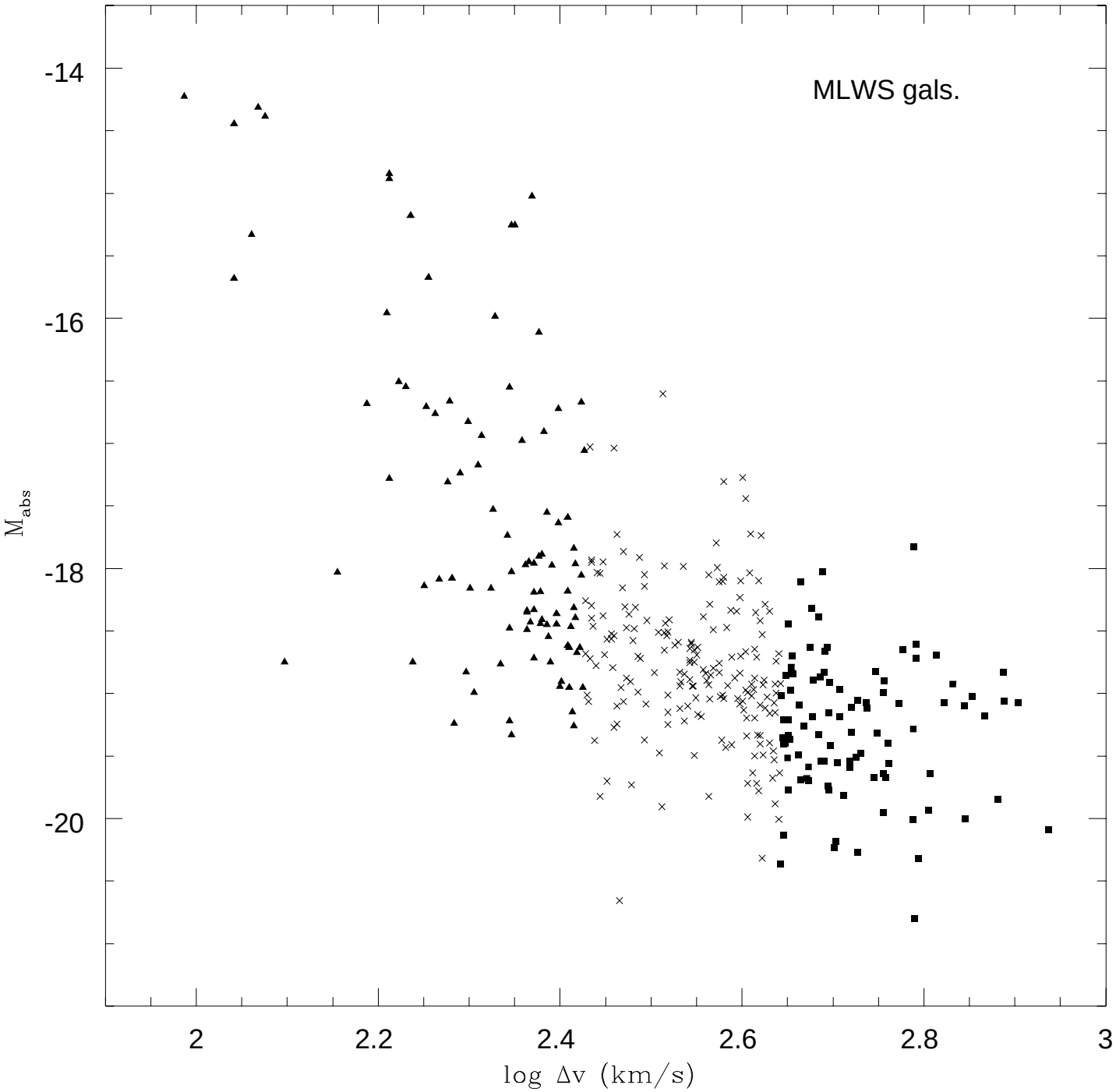
MLWS gals.
-14
-16
-18
-20
M_{abs}
2
2.2
2.4
2.6
2.8
3
log Δv (km/s)

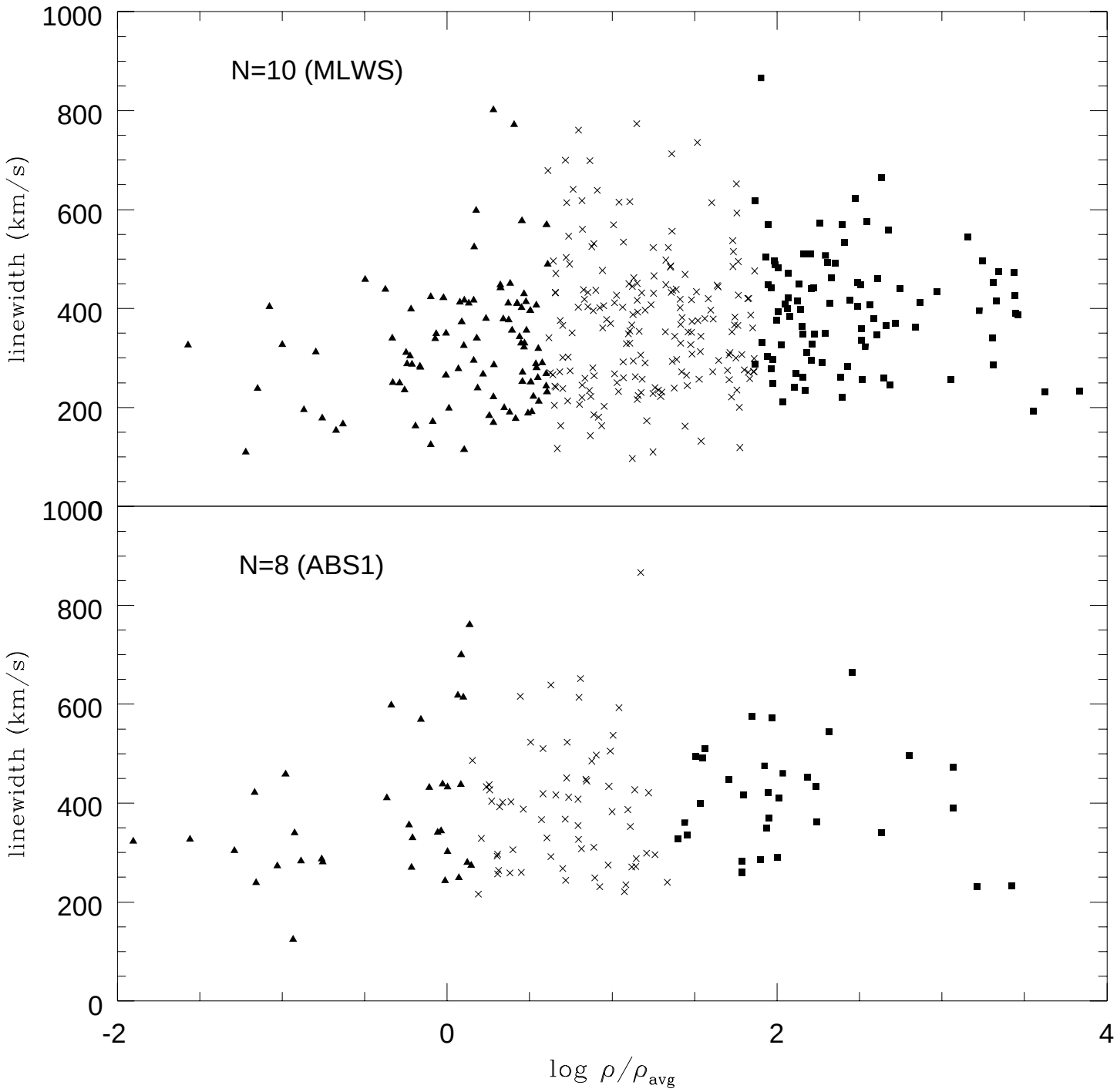
N=10 (MLWS)
N=8 (ABS1)
linewidth (km/s)
linewidth (km/s)
1000
800
600
400
200
1000
800
600
400
200
0
-2
0
2
4
log ρ/ρ_{avg}

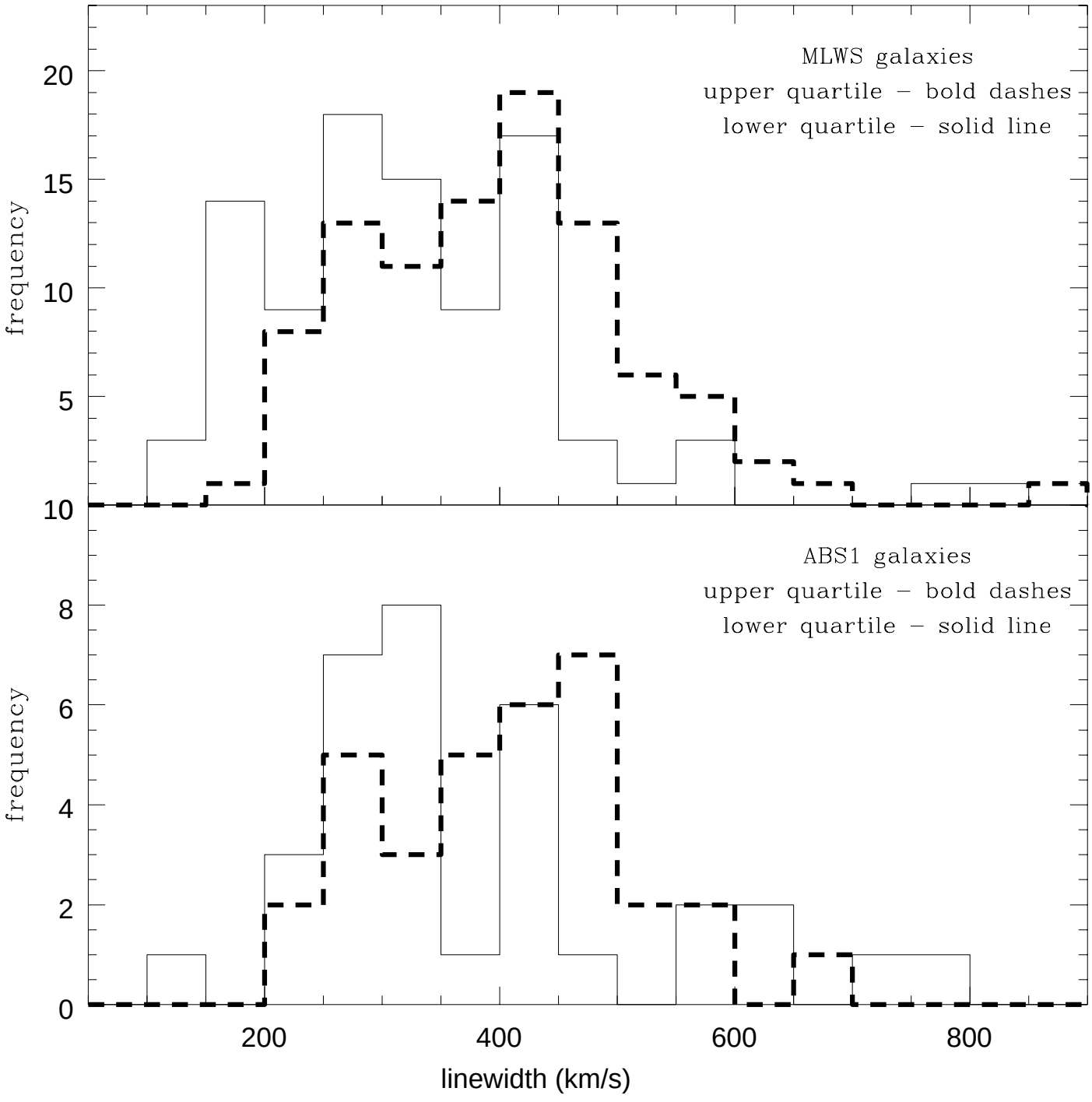
MLWS galaxies
upper quartile – bold dashes
lower quartile – solid line
frequency
20
15
10
5
10
ABS1 galaxies
upper quartile – bold dashes
lower quartile – solid line
frequency
8
6
4
2
0
200
400
600
800
linewidth (km/s)

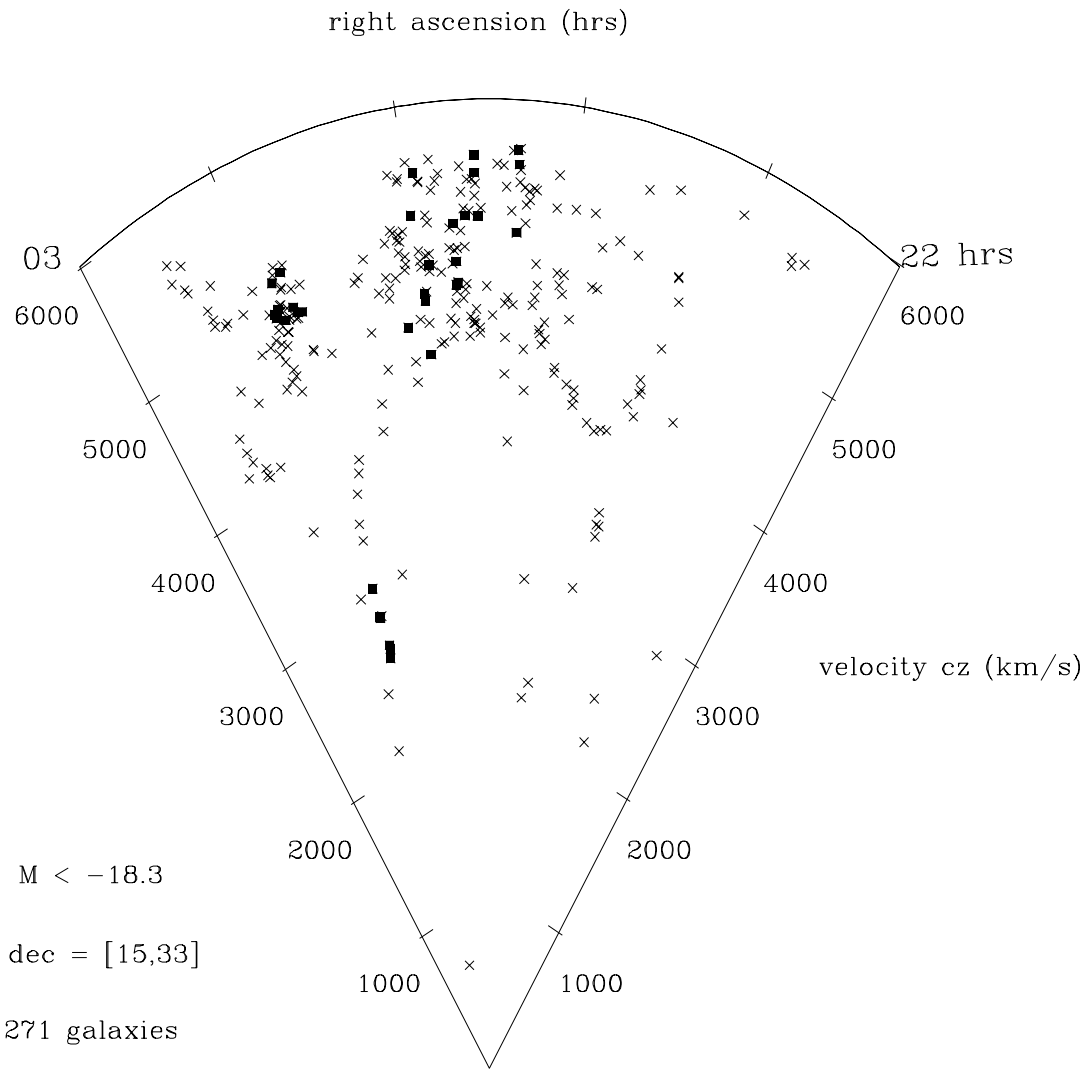
right ascension (hrs)
03
22 hrs
6000
5000
4000
3000
2000
1000
velocity cz (km/s)
M < −18.3
dec = [15,33]
271 galaxies

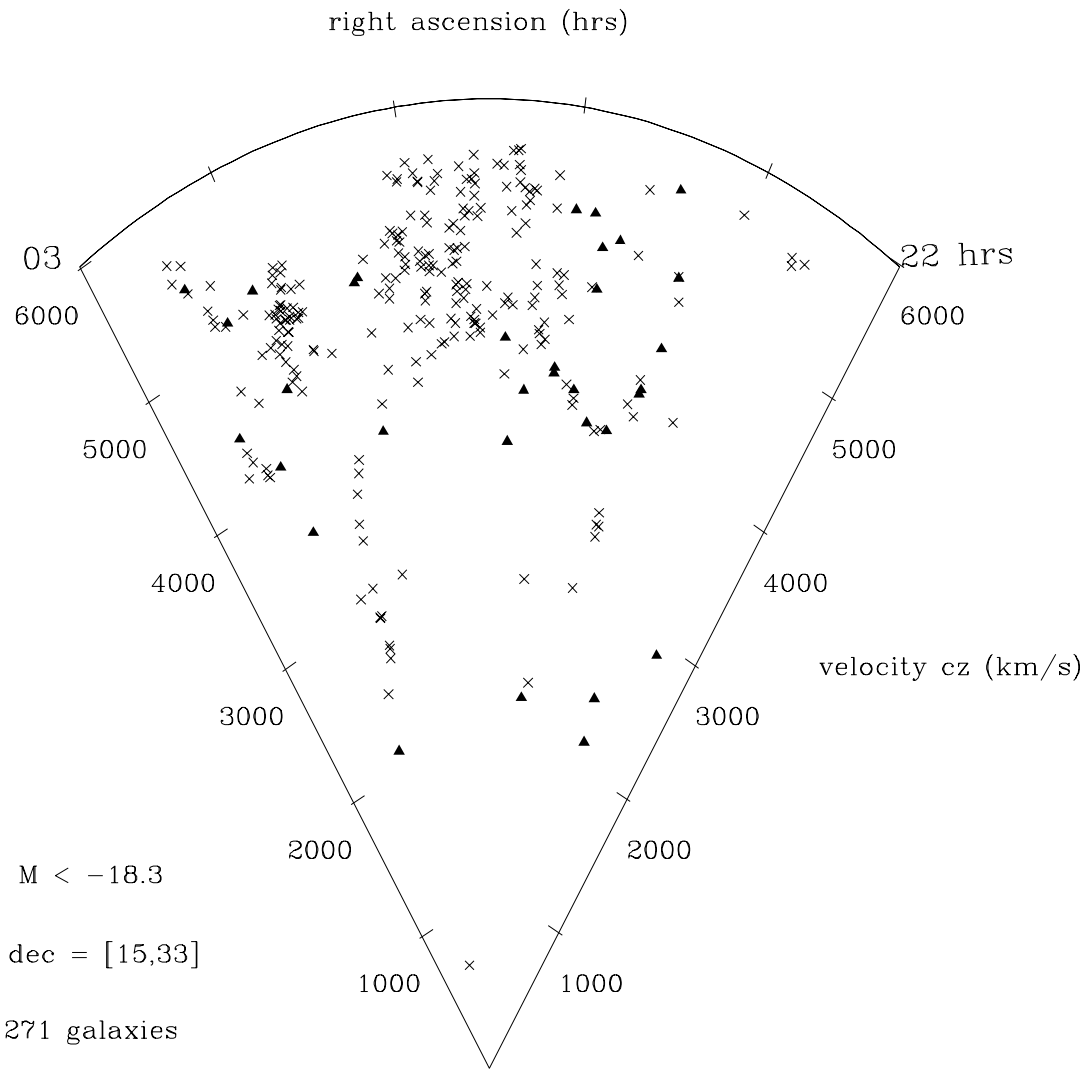
right ascension (hrs)
03
22 hrs
6000
5000
4000
3000
2000
1000
velocity cz (km/s)
M < −18.3
dec = [15,33]
271 galaxies

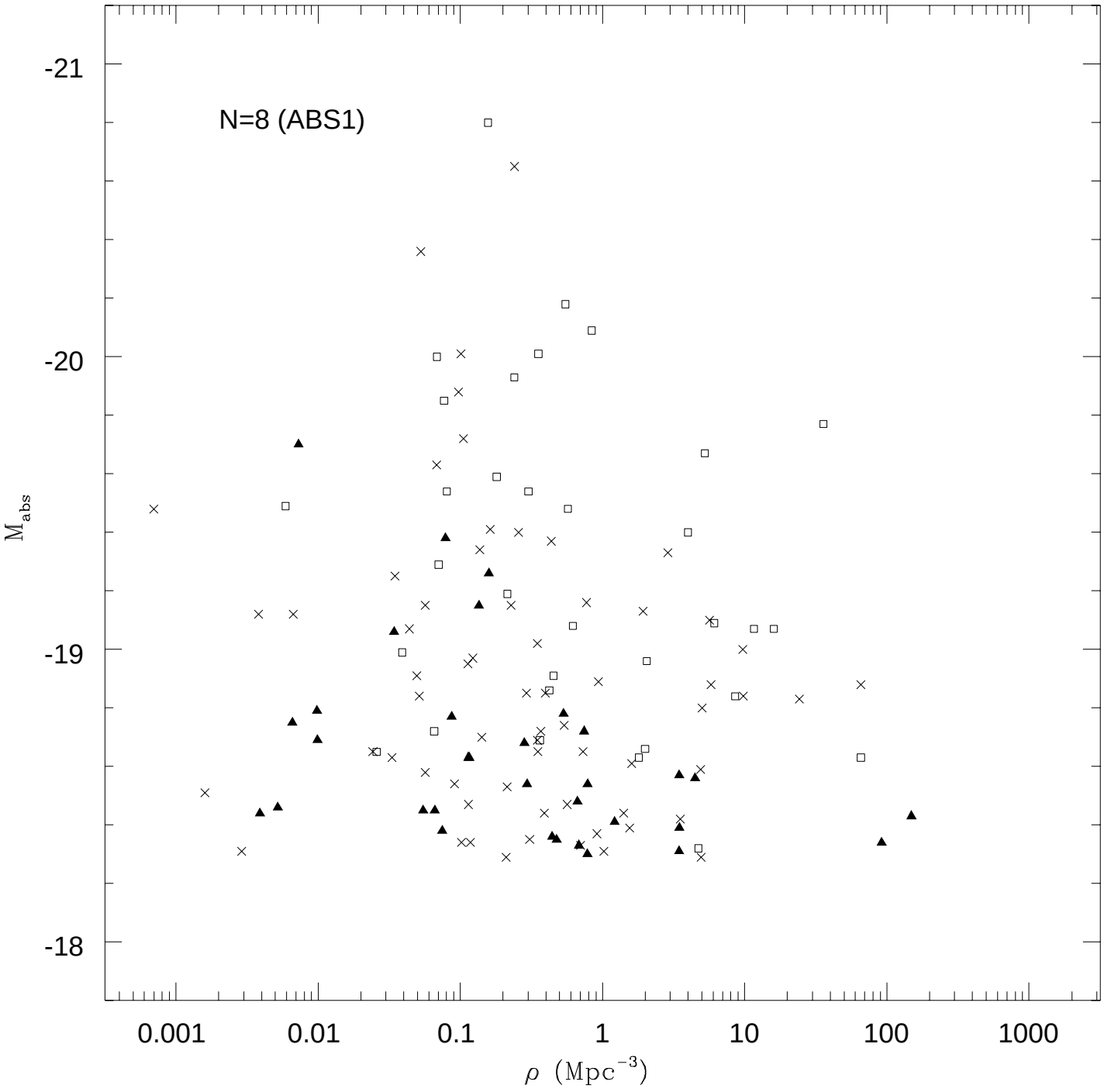
N=8 (ABS1)
-21
-20
-19
-18
M_{abs}
0.001
0.01
0.1
1
10
100
1000
ρ (Mpc^{-3})